Printable organic TFT technologies for FPD applications

Masahiko Ando[1, 2]
[1]Adavanced Research Laboratory, Hitachi, Ltd.
1-1, Omika-cho 7-chome, Hitachi-shi, Ibaraki-ken, 319-1292, Japan
[2]Optoelectronic Industry and Technology Development Association (OITDA)
1-1, Higashi 1-Chome, Tsukuba-shi, Ibaraki-ken, 305-8565, Japan

Abstract

We have recently developed new organic TFT technologies such as self-aligned self-assembly (SALSA) process and a high-resolution color active-matrix LCD panel. A new method to realize high-resolution printable organic TFT array to drive active-matrix flat-panel display will be discussed.

1. Introduction

There is increasing demand for low-cost, large-area arrays of thin-film transistors (TFTs) to supply the huge number of electronic devices such as paper-like displays and radiofrequency identification tags, which are required for new forms of ubiquitous and mobile communication. Organic TFTs have potential as building blocks for such electronic devices based on flexible substrates since they can be manufactured using inexpensive solution processing and direct printing process rather than expensive vacuum deposition and photolithographic patterning [1]. However, their practical application requires the development of novel printing techniques and device structures that provide accurate definition of device patterns with micrometer resolution without highly complex processing. At the same time, assembly process of organic TFTs with other devices such as flat-panel display (FPD) must also be developed.

Based on the background described above, we have recently developed a simple fabrication process for a self-aligned organic TFT and a high-resolution active-matrix color liquid crystal display (LCD) driven by organic TFT array [2]-[4].

2. Self-Aligned Self-Assembly TFT Process

A key point of the TFT fabrication process is patterning the hydrophobic self-assembled monolayer (SAM) by a back-substrate exposure technique using the lower (gate) electrode as a photolithographic mask. The optically patterned SAM not only defines the self-aligned position of the solution-processed upper electrodes, but it also selectively orders the structure of the semiconductor molecules deposited on it. Therefore, both the electrodes and semiconductor film are substantially self-aligned to each other. We call this process "*self-aligned self-assembly (SALSA)*".

A schematic illustrating the TFT fabrication process and structure is presented in **Fig. 1**. An ordinary bottom-gate and bottom-contact structure was used; the gate electrode, gate insulator and source and drain electrodes were stacked, and then the semiconductor film was formed to complete the device. Stripes of gate electrodes of sputtered Cr, 120-nm thick, were patterned on a quartz-glass substrate, and a silicon dioxide

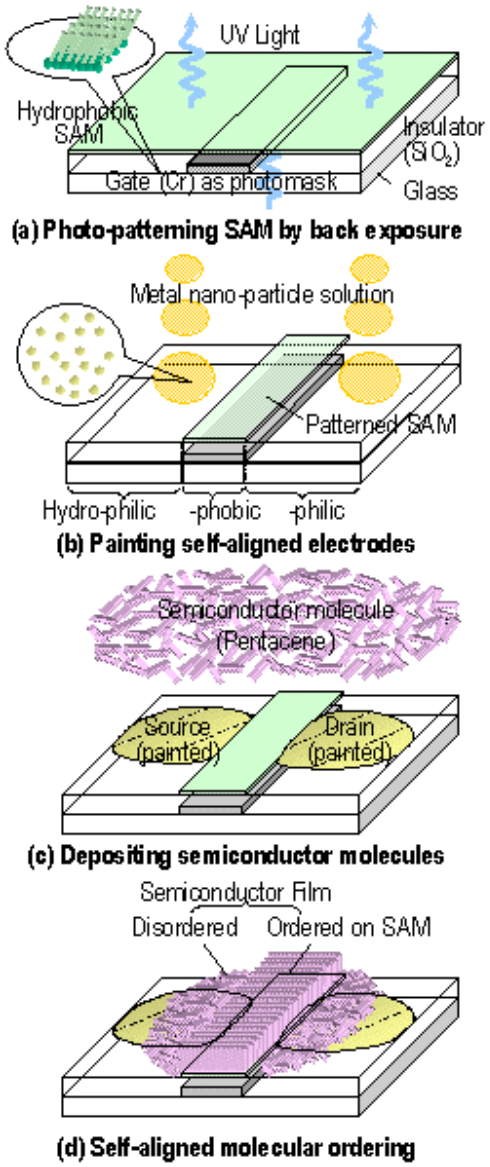

Fig.1. Self-aligned self-assembly TFT process.

(SiO_2) film, 400-nm thick, was deposited with a plasma-enhanced chemical vapor deposition system by using a mixture of TEOS (tetra-ethoxy-silane) and O_2 gas. A hydrophobic

SAM (perfluoro-polymer) was dip-coated on the substrate, and this was then exposed from the back by using a low-pressure mercury lamp to remove the SAM from the surface area of the SiO_2 not shadowed by gate electrodes. Source and drain electrodes were patterned by painting a water-based solution of silver (Ag) nano-particles on the hydrophilic stripes interposed between the residual hydrophobic stripes just above the gate electrodes. The substrate was baked in vacuum at 120℃ for 20 minutes. Finally, pentacene molecules were deposited with thermal evaporation without heating to make an organic semiconductor film, 50-nm thick. The TFT characteristics were measured in a vacuum chamber with a semiconductor characterization system (Keithley 4200-SCS). Atomic force microscopy was used to measure the morphology of pentacene films deposited on the hydrophobic and hydrophilic areas and the TFT performances were compared.

UV exposure time dependence of contact angle of water droplets was measured on the substrate surface as shown in **Fig.2**. While the contact angle of shadowed surface keeps a constant value at 110 ° , that of exposed and back surfaces decreased to less than 30 ° with a UV exposure time of 30 minutes.

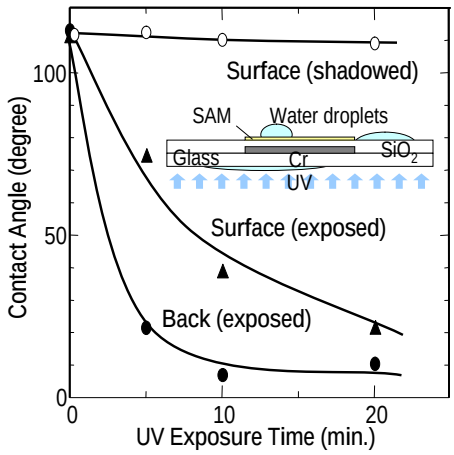

Fig.2. Photo-patterning of SAM with back exposure.

A planar view of the Ag electrodes painted on the optically patterned SAM and schematic illustrating the self-alignment mechanism are shown in **Fig. 3**; the widths of the hydrophilic lines are 300-μm and the hydrophobic spaces are 800-μm. The upper Ag electrodes are completely self-aligned to the lower Cr electrodes with no overlap. The perimetrical rim bulges uniformly. This bulge is probably caused by "the coffee stain effect" [5], in which Ag nano-particles dispersed in a water solution flow outward and aggregate at the edge during drying to form a bulge. This specific shape indicates that the contact line of the Ag solution was pinned at the adjacent SAM situated just above the lower Cr electrode to make a self-aligned structure. This pinning effect is critical to forming the self-aligned electrodes. The pinning can be explained as

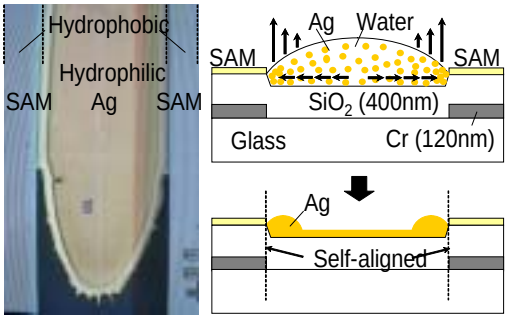

Fig.3. Mechanism of self-alignment in painted electrode.

follows. (1) The hydrophilic lines separated by hydrophobic spaces are filled with a controlled amount of Ag solution to get the contact angle of about 45 ° , which is higher than the minimum value for a hydrophilic-free surface (about 30 °). The volume of solution is sufficient to maintain the outward flow to the contact lines adjacent to the hydrophobic edge during the drying process. (2) The hydrophilic sidewalls of the SiO_2 insulator at the heterogeneous boundary are naturally formed because the lower electrodes (120-nm thick) push up the hydrophobic areas, and this causes the contact line of the drying Ag solution to remain pinned. This latter explanation is consistent with the results of sub-micrometer dewetting that were obtained using a mesa-structured hydrophobic barrier [6]. The minimum sizes of the painted electrodes' lines and spaces were 7-μm and 3-μm, respectively, and this indicates that organic self-aligned TFTs with a 3-μm channel length potentially can be fabricated using this method. High-resolution, printable electrodes are possible since the hydrophobic SAM is quite thin, about 1-nm thick, which is approximately three orders of magnitude thinner than the photoresist currently used for this kind of self-alignment process. Another advantage of using hydrophobic SAM is that the optical patterning is a completely dry process, which is much simpler than the wet chemical process used for photoresist patterning.

Effects of SAM on transfer characteristics and morphology of semiconductor films in two kinds of TFTs are shown in **Fig. 4**. Here, pentacene deposited film and F8T2 (poly-fluorene-co-bithiophene) spin-coated films were used as semiconductor layers. In the case of pentacene with SAM, the field-effect mobility and threshold voltage were 0.15 cm^2/Vs and -5 V, respectively. The obtained on/off current ratio of 10^5 is reasonably high for devices without passivation. In contrast, without SAM, the on-current was decreased and the off-current was simultaneously increased, and the field-effect mobility and on/off ratio respectively were reduced by a half and approximately one order of magnitude. Atomic force microscopic images (inset) show that the average grain size of the pentacene film was increased with SAM treatment from about 100 nm to more than 200 nm, and this was the reason for the improvement in the field-effect mobility and on/off current ratio [7]. The grain size of the pentacene film deposited on the region outside the gate electrode was smaller because the SAM

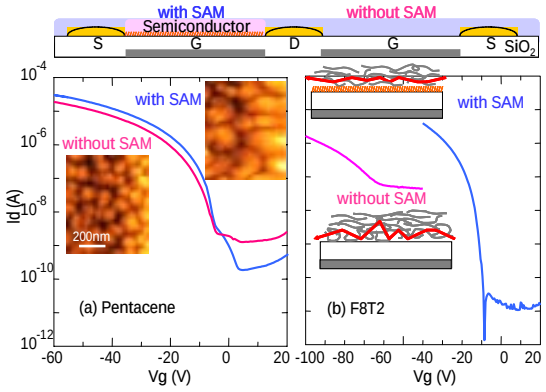

Fig.4. Effect of patterned SAM on TFT performance.

was removed from this region by exposing the back of the substrate. The increase in field-effect mobility resulting from SAM treatment in this study was relatively small compared with that reported when thermal oxide was used as a gate insulator [8]. This may be due to the surface roughness of SiO_2 films deposited at a high deposition rate of 0.5 nm/s and the rough surface of the Cr gate electrodes. These rough surfaces may have induced a large number of nucleations for small crystalline grains and prevented the diffusion-limited grain growth of the dendritic structure that is usually expected on a smooth surface. In the case of F8T2 with SAM, the field-effect mobility and threshold voltage were approximately 0.01 cm^2/Vs and -10 V, and the on/off current ratio was more than 10^5. In contrast, without SAM, the field-effect mobility was decreased more than two orders of magnitude with large threshold-voltage shift and current crowding. The same kind of mobility enhancement has already been reported elsewhere for solution-processed polymer semiconductor film [9]; the authors of that report suggest that local interaction between the polymer and SAM should modify the alignment of polymer, as is shown in the insets of Figure 4, to improve the electrical characteristics.

These results indicate that the SAM functions not only in patterning solution-processed source and drain electrodes but also in ordering the self-assembled structure of a semiconductor film. Both of these are self-aligned to the gate electrode initially formed on the substrate and are used as a photomask for patterning the SAM. This fully self-aligned structure and process are much simpler than those used to make amorphous silicon TFTs, which require complicated and expensive processes such as lift-off or ion-doping. The system does not require precise alignment, although further refinement will be necessary to combine the process with the recently developed use of high-definition inkjet printing for electrodes and solution-processed semiconductor and insulator films for organic TFTs.

3. Active-Matrix LCD with Organic TFT

We successfully demonstrate a color LCD with resolution at 80 ppi (pixels per inch), the highest resolution color display with organic TFT ever reported (**Fig.5**). Color moving images

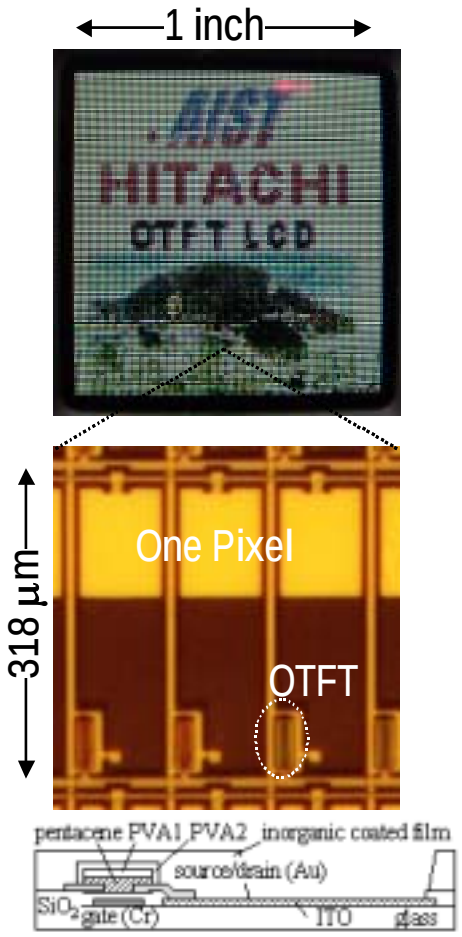

Fig.5. Organic TFT LCDpanel.

Display Size	1.4 inches diagonal
Resolution	80 ppi
Pixcel Number	80×80
Pixcel Size	318×318 μm^2
TFT W/L	50 μm / 5 μm
Mobility	0.02cm^2/Vs
Signal Voltage	10 V
Gate Voltage	35 V
Frame Frequency	60 Hz

Table.1. Specification of the OTFT-LCD panel

can be displayed with driving frequency at 60 Hz. Specifications of the display are summarized in **Table.1**.

Plain view and cross section of the TFT pixel are shown in **Fig.5**. The organic TFT array is protected with newly developed hybrid passivation layers without seriously degrading the TFT performance even after assembled with liquid crystal layer. Channel width and length of the TFT are 50 μm and 5 μm, respectively. We use a conventional bottom gate and bottom contact structure compatible with the SALSA process shown in the previous section. In order to reduce contact resistance, R_C, between semiconductor film and source and drain electrodes, taper angle of these electrodes was increased by optimizing the lift-off process conditions [10]. The effect is clearly shown in **Fig.6**. The field-effect mobility at 0.04 cm^2/Vs with channel length at 5 μm is obtained without suffering from the effect of R_C. Passivation for semiconductor is made of three layers; the first

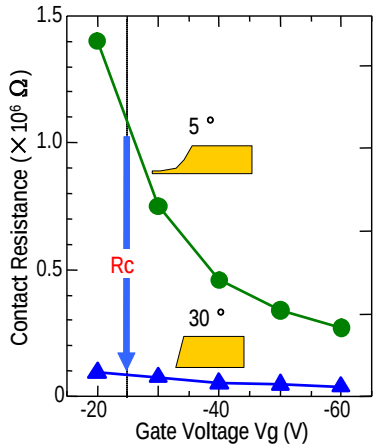

Fig.6. Effect of taper angle of electrode on contact resistance.

photosensitive poly vinyl alcohol (PVA) layer for patterning semiconductor film; the second photosensitive PVA for capping semiconductor for preventing it from peeling from the surface of gate insulator; the third soluble inorganic layer for preventing TFT from degradation after assembled with LCD. These three layers are coated in turn on the TFT backplane. The first PVA layer can be omitted if semiconductor is directly patterned using printing process. Transfer characteristics of TFT before and after passivation are shown in **Fig.7**. Passivation decreases both on and off current which transport the surface of semiconductor as a leakage current. Field-effect mobility at 0.02 cm^2/Vs and on/off current ratio more than 10^5 is shown at a relatively low applied voltage of 20 V. The switching performance does not degrade even after assembled with LCD. With 1.4 inches diagonal size, 80 x 80 (RGB) pixel number, 318 x 108 μm^2 pixel size, and 80 ppi, it is the highest resolution color display with organic transistors ever reported.

4. Future Plan

In the present study, photolithographic steps and vacuum processes were partially used to clarify the SALSA process and to check the feasibility of organic TFT to drive active-matrix LCD. In the near future, we plan to apply the SALSA solution process to fabricate organic TFT array to drive the active-matrix LCD panel. For this challenge, device design, process, and materials are integrated to realize a high-performance and high-resolution SALSA TFT array with reliability.

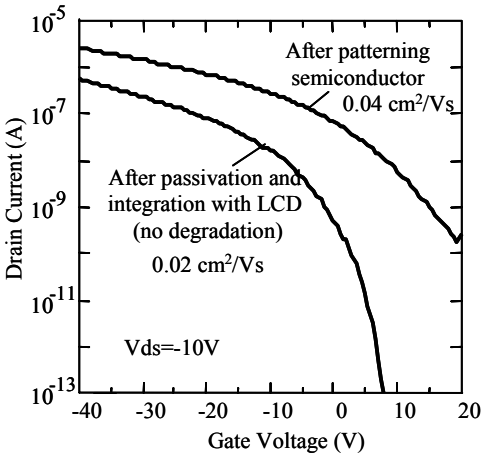

Fig7. Effect of passivation on TFT performance.

Conclusion

We have recently developed a simple fabrication process for a self-aligned organic TFT and a high-resolution active-matrix color liquid crystal display (LCD) driven by organic TFT array. These results indicate that organic TFT has potential to meet the requirement for future high-definition, high-performance, printable, organic thin-film transistors without requiring a conventional photolithographic process to drive active-matrix flexible sheet displays such as electronic papers or electronic posters.

Acknowledgements

This work is partially supported by the "Advanced Organic Device Project" under a contract between OITDA, National Institute of Advanced Industrial Science and Technology (AIST), and the New Energy and Industrial Technology Development Organization (NEDO).

References

[1] H. Sirringhaus, T. Kawase, R. H. Friend, T. Shimoda, M. Inbasekaran, W. Wu, and E. P. Woo, Science **290**, 2123 (2000).
[2] M. Ando et al., Ext. Abst. SSDM03 (Tokyo, Sept. 16-18, 2003), p. 222.
[3] M. Ando et al., Appl. Phys. Lett. 85(10), 1849(2004).
[4] M. Kawasaki et al., AM-LCD'04 Digest (Tokyo, Aug. 25-27, 2004), p.25.
[5] R. D. Deegan, O. Bakajin, T. F. Dupont, G. Huber, S. R. Nagel, and T. A. Witten, Nature **389**, 827 (1997).
[6] J. Z. Wang, Z. H. Zheng, H. W. Li, W. T. S. Huck, and H. Sirringhaus, Nature Materials **3**, 171 (2004).
[7] Y.-Y. Lin, D. J. Gundlach, S. F. Nelson, and T. N. Jackson, IEEE Trans. Elec. Dev. **44** 1325 (1997).
[8] D. Knipp, R. A. Street, A. Voekel, and J. Ho, J. Appl. Phys. **93**, 347 (2003).
[9] A. Salleo, M. L. Chabinyc, M. S. Yang, and R. A. Street, Appl. Phys. Lett. **81**, 4383 (2002).
[10] M. Kawasaki et al., Ext. Abst. SSDM03, (2003), p.690.